ChemistryOPEN

Supporting Information

Porphyrinic Ionic Liquid Dyes: Synthesis and Characterization

Kai Li,[a, c] Hatem M. Titi,[a] Paula Berton,[a, d] and Robin D. Rogers*[a, b, c]

open_201800166_sm_miscellaneous_information.pdf

Experimental

Chemicals

1-Ethylimidazole, 1,12-dibromododecane (98%), 1-bromododecane (>97%), potassium hexafluorophosphate (KPF_6, >99%), sodium tetrafluoroborate ($NaBF_4$, >98%), bis(trifluoromethane)sulfonimide lithium salt ($LiNTf_2$, 98%), 5,10,15,20-Tetrakis(4-hydroxyphenyl)-21H,23H-porphine (TOHPP, 97%), 5,10,15,20-Tetra(4-pyridyl)porphyrin (T^4PyP), potassium carbonate (K_2CO_3, 99%), 9, 10-dimethylanthracene (DMA, 99%), *meso*-tetraphenylporphyrin (TPP, 99%), chloroform-*d* ($CDCl_3$-*d*) and dimethyl sulfoxide-d_6 (DMSO-d_6) were purchased from Sigma-Aldrich (Milwaukee, WI). Dimethylformamide (DMF), methanol (MeOH), dichloromethane (DCM), tetrahydrofuran (THF), and ethyl acetate were purchased from Fisher Scientific (Montreal, QC). All chemicals were used as received unless otherwise stated.

Synthetic procedure

*Synthesis of 1-(12-bromododecyl)-3-ethylimidazolium bromide (**a**)*

A modified synthetic procedure of **a**[1]: 2.4 g 1-ethylimidazole (25 mmol) in 20 mL DCM was added to a solution of 1,12-dibromododecane (25 g, 78 mmol) in DCM at room temperature. The reaction mixture was refluxed at 50 ºC for 18 h. After reaction, DCM was evaporated with a rotoevaporator, and the unreacted 1, 12-dibromododecane was washed out with 200 mL hexane. The resultant viscous sample was purified with silica column chromatography (DCM/MeOH = 7/1). After solvent evaporation, 4.5 g yellowish liquid was obtained and crystalized after leaving at room temperature for 24 h. Yield: 56%. ^{1}H NMR (500 MHz, $CDCl_3$-*d*) δ 10.67 (s, 1H), 7.39 (s, 1H), 7.29 (s, 1H), 4.42 (m, 2H), 4.36 - 4.28 (m, 2H), 3.37 (t, 2H), 1.89 (m, 2H), 1.81 (m, 2H), 1.58 (t, 3H), 1.47 - 1.17 (m, 16H). ^{13}C NMR (126 MHz, $CDCl_3$-*d*) δ 137.39, 121.63, 121.42, 50.20, 45.35, 34.14, 32.80, 30.33, 29.48 - 29.25, 28.97, 28.71, 28.13, 26.27, 15.66.

Synthesis of TOHPP salts

1: 0.734 g **a** (1.73 mmol) and 0.235 g TOHPP (0.346 mmol) were separately dissolved in 20 mL DMF. Then the solutions were mixed under N_2 flow and stirred in a 200 mL two neck flask. The resulting mixture was bubbled with N_2 for 30 min and 3.247g (23.5 mmol) K_2CO_3 was added during a continuous N_2 bubbling for another 30 min. The temperature was then increased to 80 ºC

and reacted for 18 h. After reaction, the solvent was removed using rotoevaporator at 80 ^{o}C. The product was re-dissolved in 50 mL DCM and filtered with a Buchner funnel to remove the salts. The DCM was removed from the filtrate by rotoevaporator and the resultant compound was washed with 300 mL ethyl acetate to remove unreacted **a**. The product was further washed with 500 mL cold deionized (DI) water to remove any unreacted **a**. Yield: 71%. ^{1}H NMR (500 MHz, DMSO-*d*$_6$) δ 9.20 (d, 4H), 8.86 (s, 8H), 8.11 (d, 8H), 7.81 (m, 8H), 7.37 (d, 8H), 4.27 (t, 7H), 4.22 - 4.13 (m, 17H), 1.92 (m, 8H), 1.81 (m, 8H), 1.58 (m, 8H), 1.50 - 1.18 (m, 81H). ESI-HRMS positive ion, calculated for $[C_{112}H_{154}O_4N_{12}]^{4+}$, m/z 432.8048 ($M^{4+}$); found 432.88043, ESI-HRMS negative ion, calculated for Br^-, m/z 78.9183; found 78.9173.

3: 76.5 mg **1** (0.037 mmol) was added to an Erlenmeyer flask containing 150 mL DI water, and the mixture was magnetically stirred until complete dissolution, after which 68 mg KPF_6 (0.37 mmol) was added. The mixture was magnetically stirred at room temperature for 24 h. The solution was centrifuged (3500 rpm, 10 min, Thermo Scientific Sorvall Legend XF, Waltham, MA), and the precipitate was washed three times with 150 mL DI water and freeze dried for 24 h using a freeze dryer (Freezone 2.5, Labconco, Kansas City, MS). 63 mg product was obtained. Yield: 73%. ^{1}H NMR (500 MHz, DMSO-*d*$_6$) δ 9.19 (d, 4H), 8.86 (s, 8H), 8.11 (d, 8H), 7.80 (m, 8H), 7.37 (d, 8H), 4.22 - 4.17 (m, 24H), 1.92 (m, 8H), 1.81 (m, 8H), 1.58 (m, 8H), 1.50 - 1.18 (m, 76H), -2.88 (s, 2H). ^{19}F NMR (471 MHz, DMSO-*d*$_6$) δ -69.41, -70.92. ^{13}C NMR (126 MHz, DMSO-*d*$_6$) δ 136.09, 122.88, 122.60, 49.33, 44.68, 29.81, 29.61, 29.56, 29.49, 29.45, 29.36, 28.88, 26.23, 26.03, 15.49. ESI-HRMS positive ion, calculated for $[C_{112}H_{154}O_4N_{12}]^{4+}$, m/z 432.8048 ($M^{4+}$); found 432.8059. ESI-HRMS negative ion, calculated for $[PF_6]^-$, m/z 144.9641; found 144.9633.

Similar procedures were followed for the synthesis of **2** and **4** using **1** (1 equivalent) with $NaBF_4$ and $LiNTf_2$ (10 equivalents), respectively. **2**: yield, 80%. ^{1}H NMR (500 MHz, DMSO-*d*$_6$) δ 9.19 (s, 4H), 8.86 (s, 8H), 8.11 (d, 8H), 7.80 (m, 1.6 Hz, 8H), 7.37 (d, 8H), 4.31 - 4.11 (m, 24H), 1.96 - 1.86 (m, 8H), 1.85 - 1.77 (m, 8H), 1.61 - 1.55 (m, 9H), 1.50 - 1.17 (m, 76H), -2.88 (s, 2H). ^{19}F NMR (471 MHz, DMSO-*d*$_6$) δ -148.31. ^{13}C NMR (126 MHz, DMSO-*d*$_6$) δ 136.09, 122.88, 122.60, 113.42, 68.27, 49.33, 44.68, 29.81, 29.60, 29.55, 29.49, 29.44, 29.35, 28.88, 26.23, 26.03, 15.49. ESI-HRMS positive ion, calculated for $[C_{112}H_{154}O_4N_{12}]^{4+}$, m/z 432.8048 ($M^{4+}$); found 432.8058. ESI-HRMS negative ion, calculated for $[BF_4]^-$, m/z 87.0029; found 87.0019.

4: yield, 85%. ^{1}H NMR (500 MHz, DMSO-*d*$_6$) δ 9.19 (d, 4H), 8.86 (s, 8H), 8.11 (d, 8H), 7.80 (m, 8H), 7.37 (d, 8H), 4.27 (t, 8H), 4.22 - 4.13 (m, 16H), 1.92 (m , 8H), 1.81 (m, 8H), 1.58 (m,

8H), 1.49 - 1.20 (m, 76H), -2.88 (s, 2H). ^{19}F NMR (471 MHz, DMSO-*d*$_6$) δ -78.72. ^{13}C NMR (126 MHz, DMSO-*d*$_6$) δ 136.10, 122.88, 122.60, 49.33, 44.68, 29.81, 29.60, 29.56, 29.45, 29.35, 28.88, 26.23, 26.03, 15.49. ESI-HRMS positive ion, calculated for $[C_{112}H_{154}O_4N_{12}]^{4+}$, m/z 432.8048 ($M^{4+}$); found 432.8057. ESI-HRMS negative ion, calculated for $[NTf_2]^-$, m/z 279.9173; found 279.9172.

Synthesis of T^{4}PyP salts

5: 0.618 g T^{4}PyP (1 mmol) and 2.5 g (10 mmol) 1-bromododecane were added in a 100 mL two neck round bottom flask containing 40 mL DMF under N_2. The mixture was bubbled with N_2 for 30 min to remove the air, then the temperature increased to 150 ºC and reacted for 24 h. After reaction, the solvent was removed with rotoevaporator and a black solid was obtained. The solid was dissolved in 100 mL methanol and concentrated to a highly viscous solution. Then, the methanol solution was dropped into 500 mL acetone to precipitate the sample and the precipitate was washed with 100 mL acetone twice. The sample was dried in the oven at 80 ºC for 24 h. Yield: 75%. ^{1}H NMR (500 MHz, DMSO-*d*$_6$) δ 9.66 (m, 8H), 9.24 (s, 8H), 9.08 (m, 8H), 4.97 (t, 8H), 2.30 (m, 8H), 1.66 - 1.22 (m, 72H), 0.91 - 0.81 (m, 12H), -3.08 (s, 2H). ^{13}C NMR (126 MHz, DMSO-*d*$_6$) δ 31.79, 31.17, 29.53, 29.44, 29.20, 22.58, 14.44. ESI-HRMS positive ion, calculated for $[C_{88}H_{126}N_8]^{4+}$, m/z 323.7521 (M^{4+}); found 323.7530 (M^{4+}). ESI-HRMS negative ion, calculated for Br^-, m/z 78.9183; found, 78.9174.

6: 160 mg **5** (0.01 mmol) was dissolved in 200 mL methanol in a 500 mL Erlenmeyer flask, then 430 mg (0.4 mmol) $NaBF_4$ was added. The solution was stirred at room temperature for 24 h. After reaction, methanol was remove by roto-evaporation to obtain a black solid. The solid was washed with adequate DI water to remove NaBr. The sample was freeze-dried with freeze dryer for 24 h. Yield: 95%. ^{1}H NMR (500 MHz, DMSO-*d*$_6$) δ 9.57 (d, 8H), 9.23 (s, 8H), 9.02 (d, 8H), 4.96 (t, 8H), 2.33 - 2.21 (m, 8H), 1.65 - 1.23 (m, 72H), 0.87 (m, 12H), -3.08 (s, 2H). ^{19}F NMR (471 MHz, DMSO-*d*$_6$) δ -148.32. ^{13}C NMR (126 MHz, DMSO-*d*$_6$) δ 31.79, 31.54, 29.52, 29.20, 22.58, 14.44. ESI-HRMS positive ion, calculated for $[C_{88}H_{126}N_8]^{4+}$, m/z 323.7521 (M^{4+}); found 323.7534 (M^{4+}). ESI-HRMS negative ion, calculated for PF_6^-, m/z 144.9641; found, 144.9633.

Similar procedures were used to synthesize **7** and **8** using **5** (1 equivalent) with KPF_6 and $LiNTf_2$ (10 equivalents), respectively. **7**: Yield: 90%. ^{1}H NMR (500 MHz, DMSO-*d*$_6$) δ 9.58 (d, 8H), 9.22 (s, 8H), 9.03 (d, 8H), 4.97 (t, 8H), 2.32-2.28 (m, 8H), 1.61-1.10 (m, 72H), 0.87 (m, 12H),

-3.08 (s, 2H). ^{19}F NMR (471 MHz, DMSO-d_6) δ -69.41, -70.92. ^{13}C NMR (126 MHz, DMSO-d_6) δ 31.79, 31.54, 29.52, 29.20, 22.58, 14.44. ESI-HRMS positive ion, calculated for $[C_{88}H_{126}N_8]^{4+}$, m/z 323.7521 (M^{4+}); found 323.7526 (M^{4+}). ESI-HRMS negative ion, calculated for $[BF_4]^-$, m/z 87.0029; found, 87.0019.

8: Yield: 95%. ^{1}H NMR (500 MHz, DMSO-d_6) δ 9.58 (d, 8H), 9.22 (s, 8H), 9.02 (d, 8H), 4.96 (t, 8H), 2.34 - 2.22 (m, 8H), 1.69 - 1.10 (m, 72H), 0.87 (m, 12H), -3.08 (s, 2H). ^{19}F NMR (471 MHz, DMSO-d_6) δ -78.72. ^{13}C NMR (126 MHz, DMSO-d_6) δ 31.79, 31.54, 29.52, 29.20, 22.58, 14.44. ESI-HRMS positive ion, calculated for $[C_{88}H_{126}N_8]^{4+}$, m/z 323.7521 (M^{4+}); found 323.7526 (M^{4+}). ESI-HRMS negative ion, calculated for $[NTf_2]^-$, m/z 279.9173; found 279.9179.

Characterization

Nuclear Magnetic Resonance (NMR) Spectroscopy. ^{1}H, ^{13}C, and ^{19}F NMR spectra were recorded on a Bruker AV500 (Madison, WI ^{1}H NMR, 500 MHz; ^{13}C NMR, 126 MHz; ^{19}F NMR, 471 MHz) in $CDCl_3$ or DMSO-d_6.

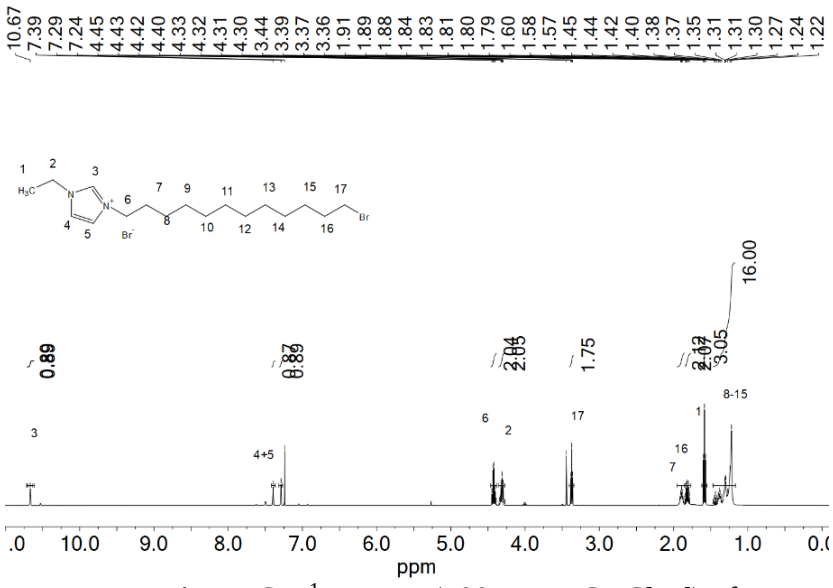

Figure S1. ^{1}H NMR (500 MHz, $CDCl_3$-d) of **a**.

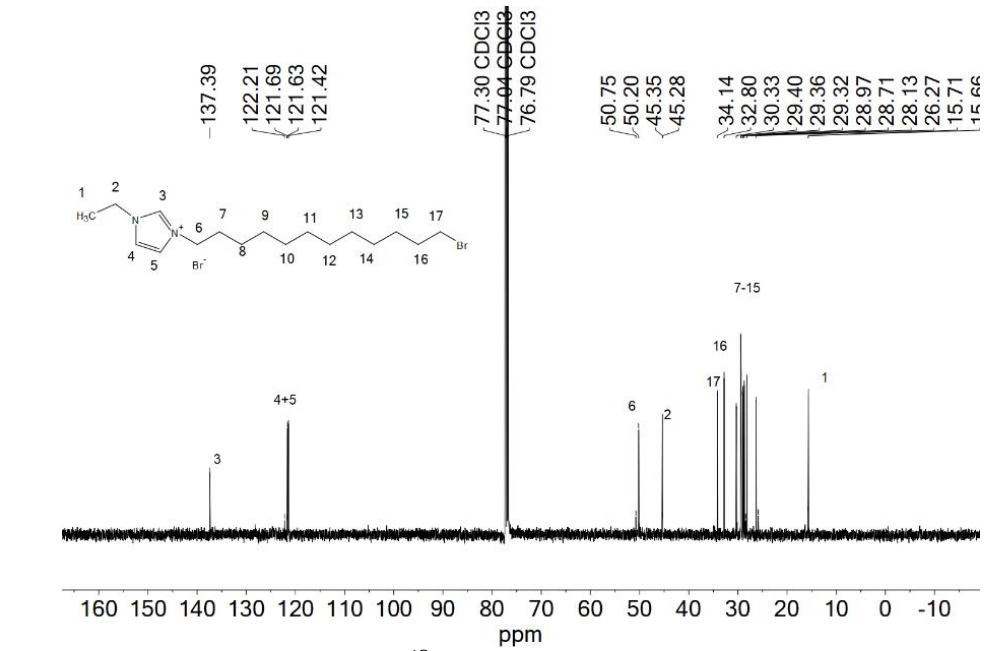

Figure S2. ^{13}C NMR (126 MHz, $CDCl_3$-*d*) of **a**.

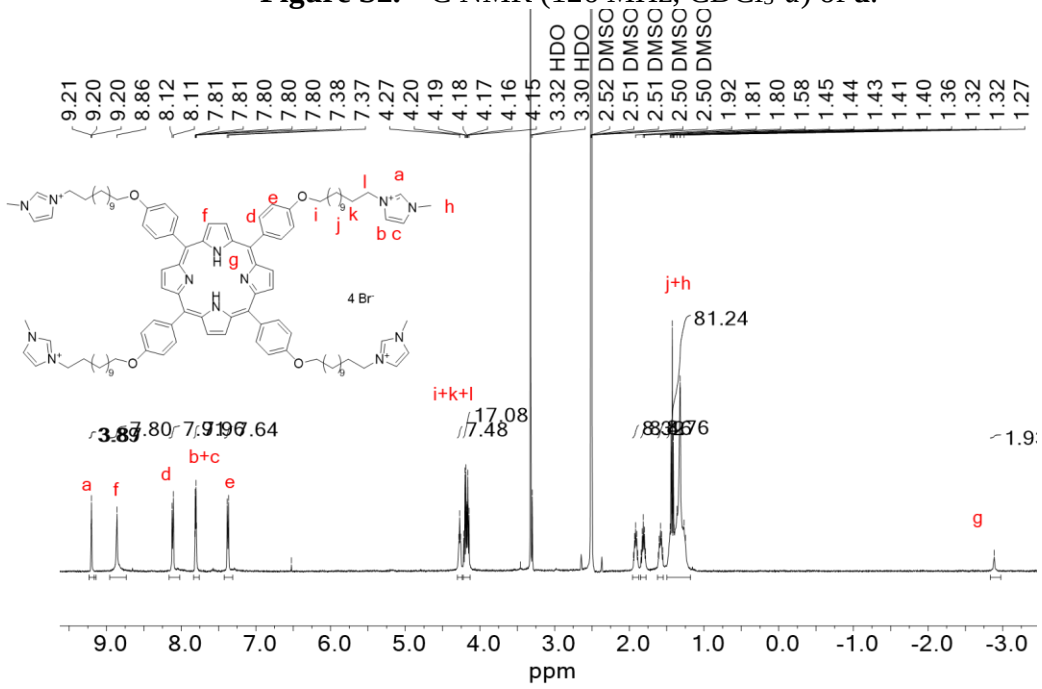

Figure S3. ^{1}H NMR (500 MHz, DMSO-d_6) of **1**.

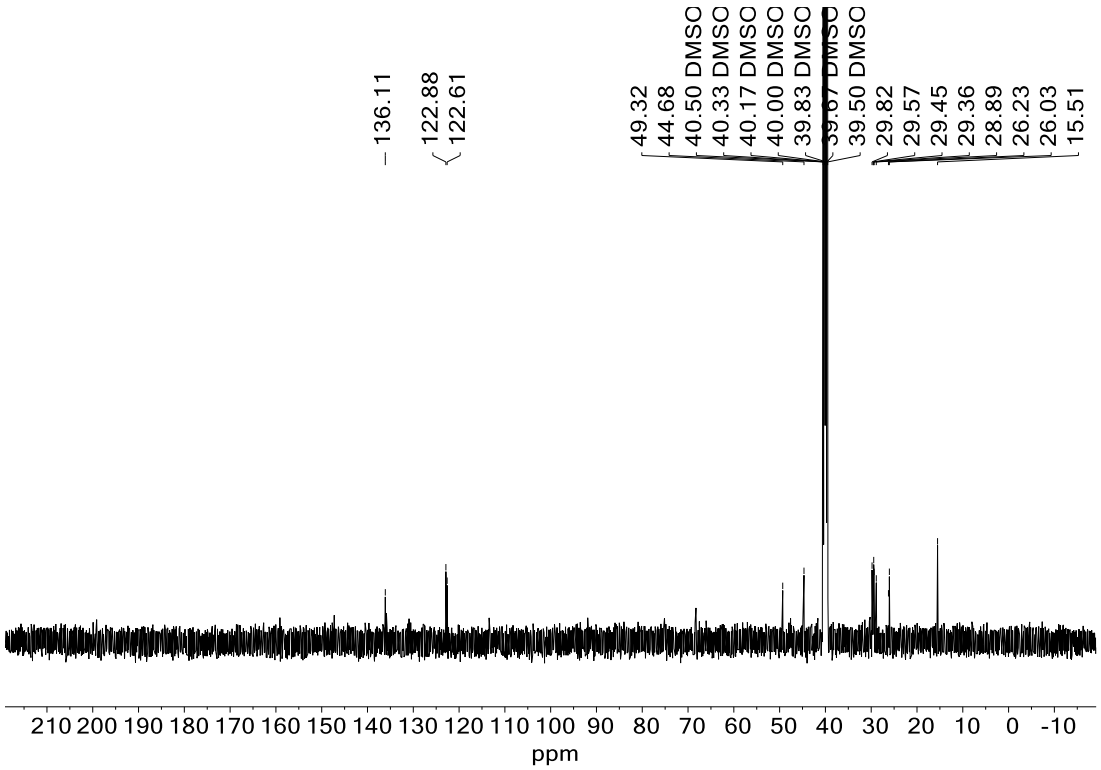

Figure S4. ^{13}C NMR (126 MHz, DMSO-d_6) of **1**.

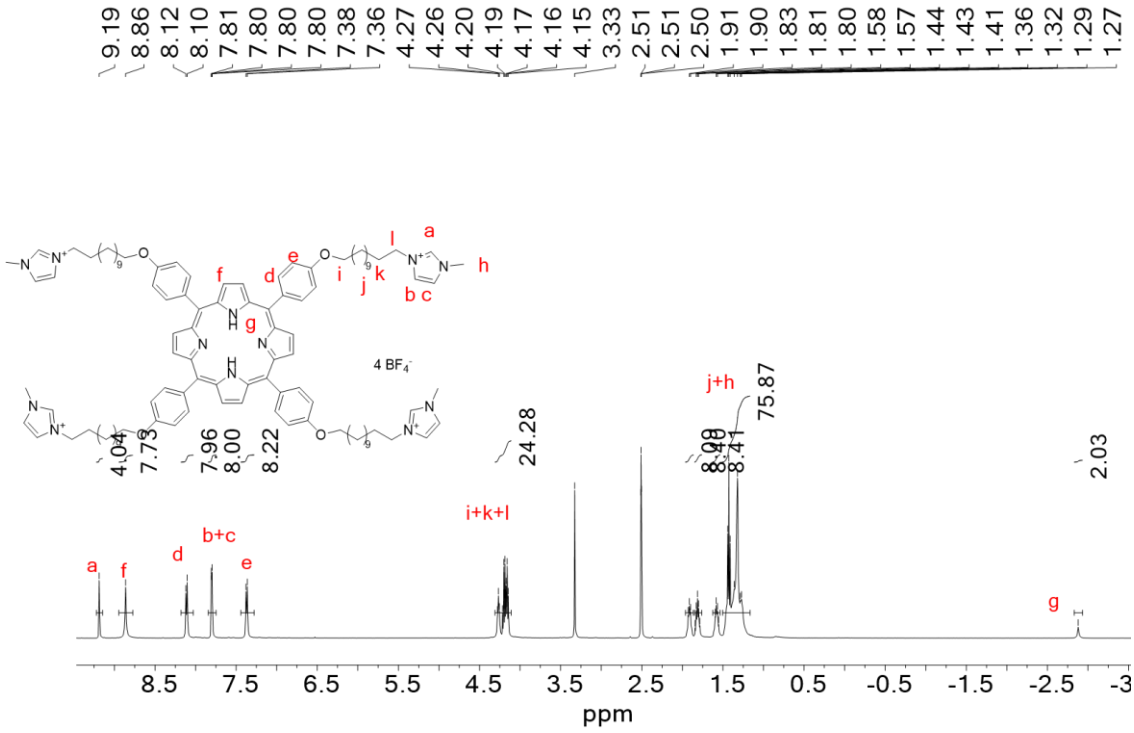

Figure S5. ^{1}H NMR (500 MHz, DMSO-d_6) of **2**.

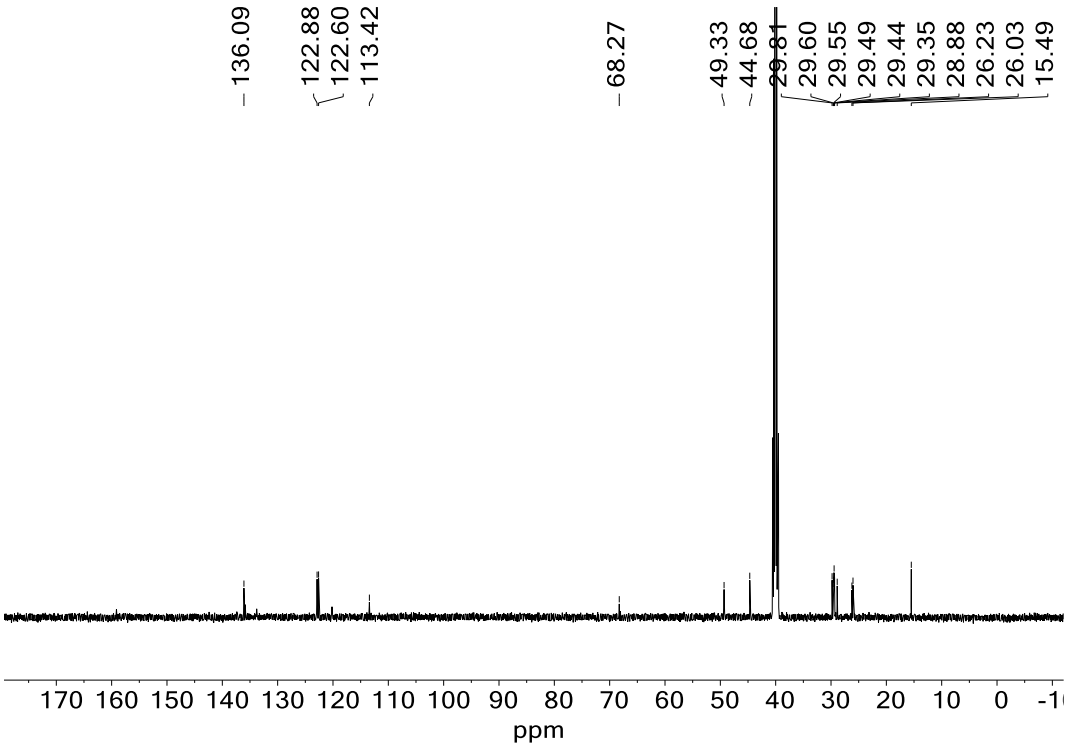

Figure S6. ^{13}C NMR (126 MHz, DMSO-d_6) of **2**.

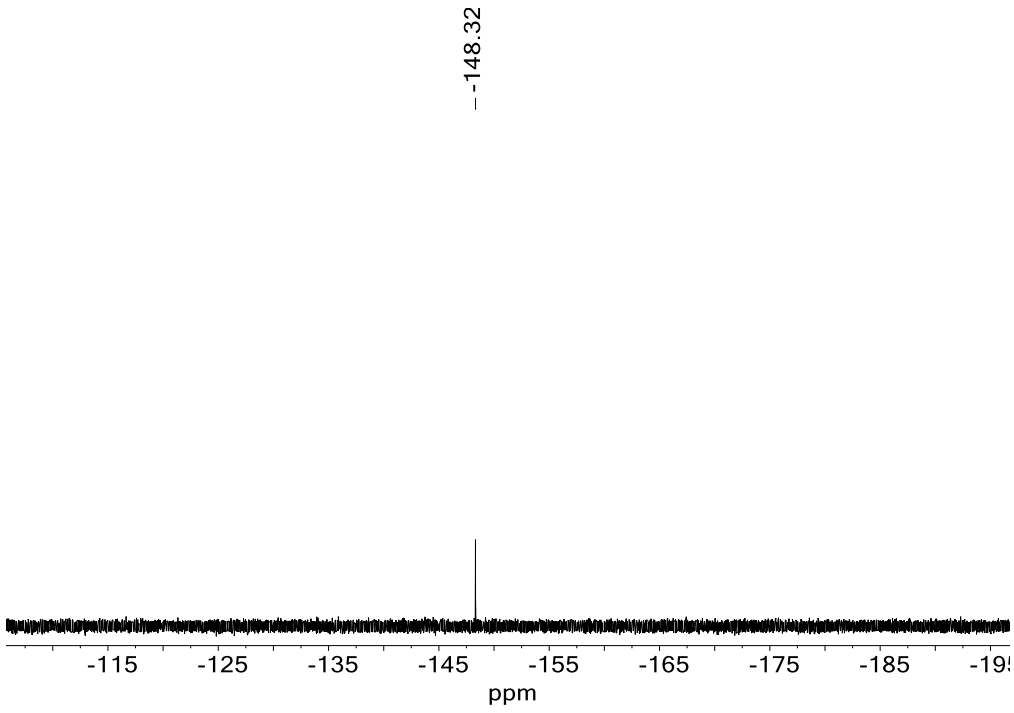

Figure S7. ^{19}F NMR (471 MHz, DMSO-d_6) of **2**.

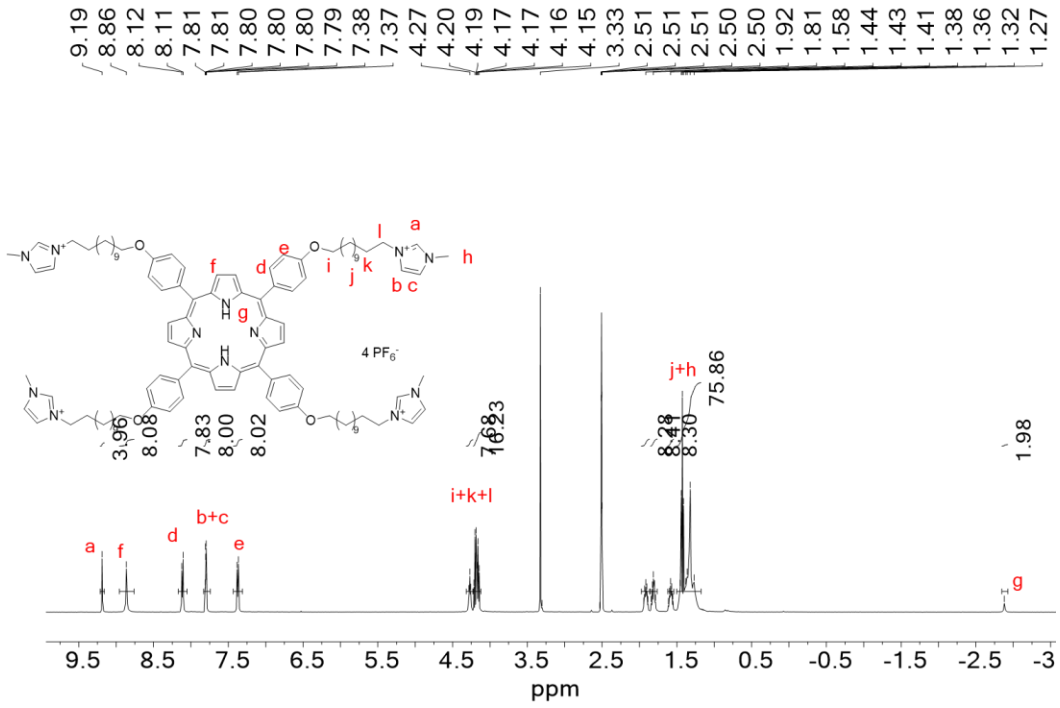

Figure S8. ^{1}H NMR (500 MHz, DMSO-d_6) of **3**.

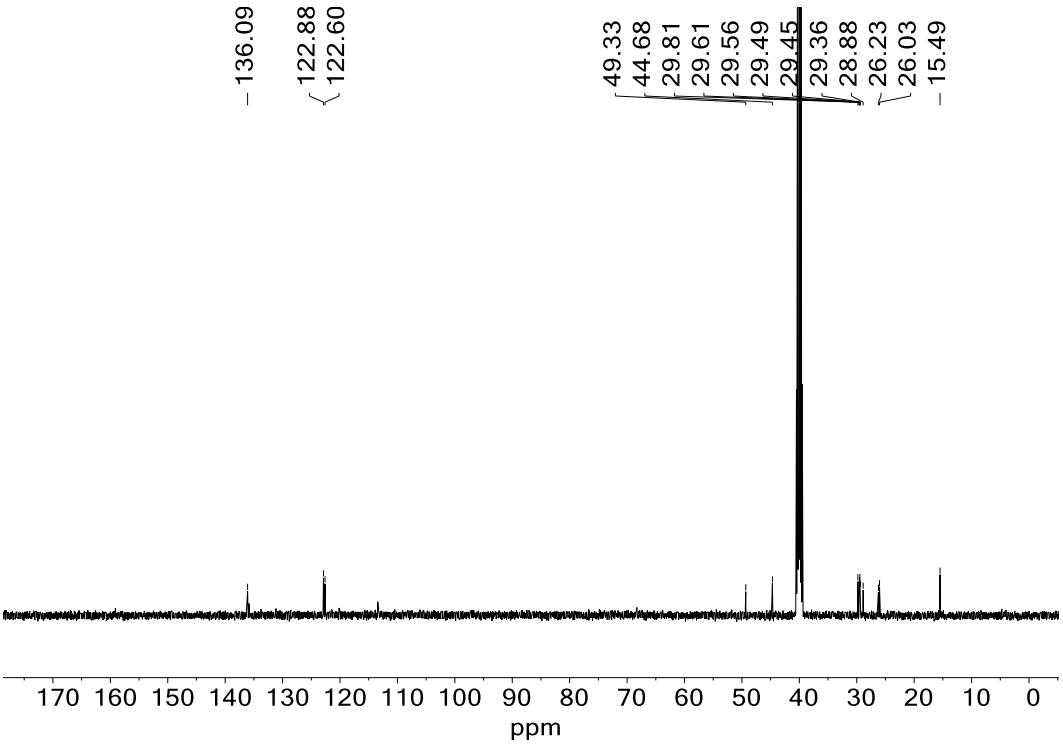

Figure S9. ^{13}C NMR (126 MHz, DMSO-d_6) of **3**.

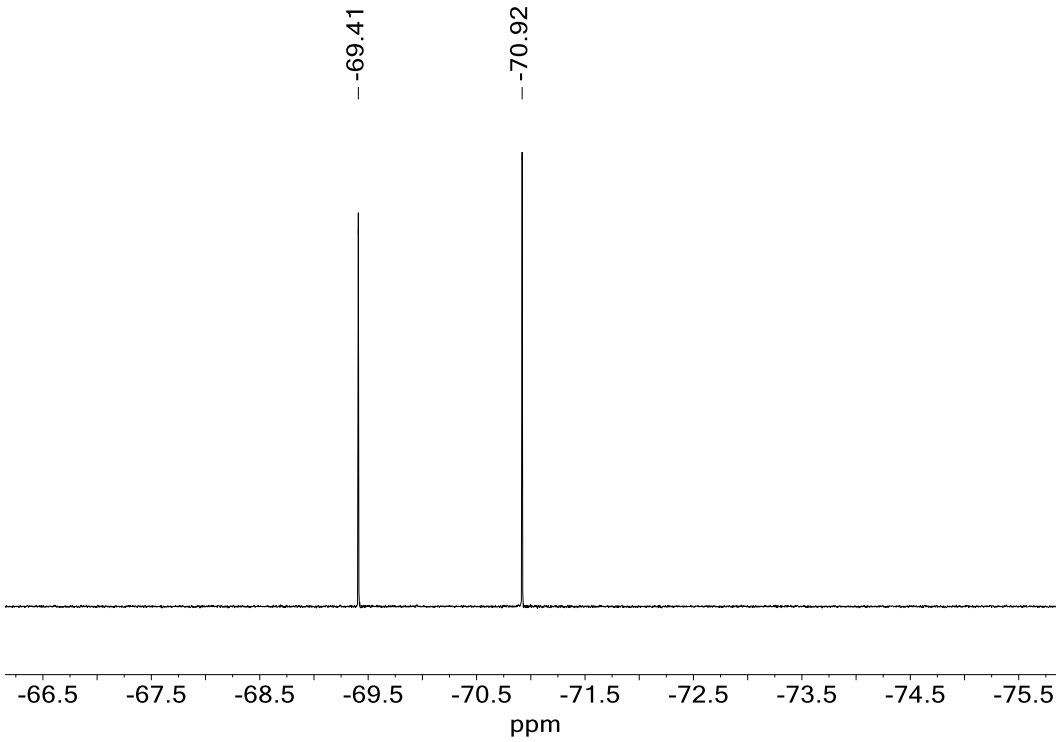

Figure S10. ^{19}F NMR (471 MHz, DMSO-*d*$_6$) of **3**.

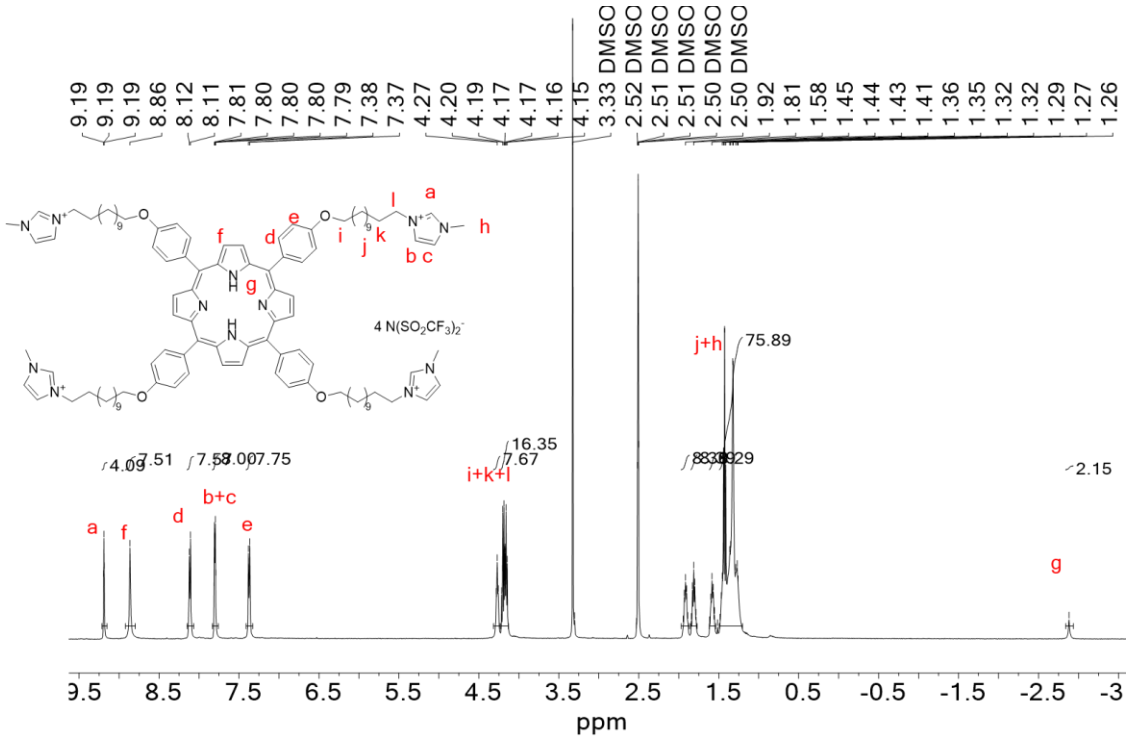

Figure S11. ^{1}H NMR (500 MHz, DMSO-*d*$_6$) of **4**.

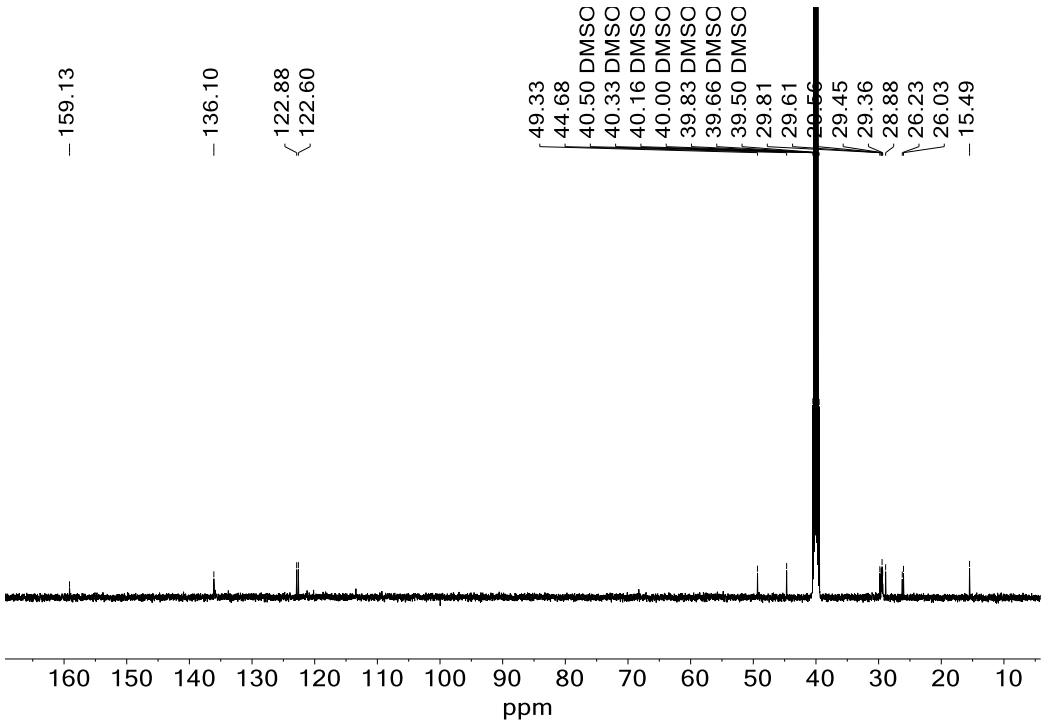

Figure S12. ^{13}C NMR (126 MHz, DMSO-d_6) of **4.**

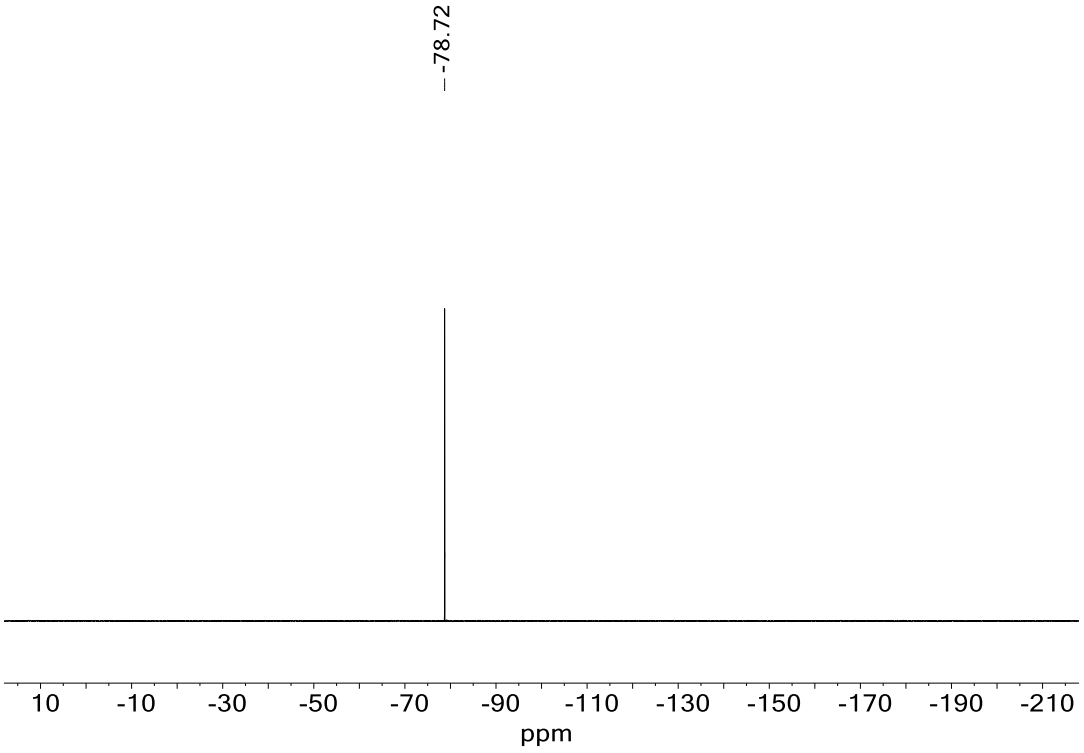

Figure S13. ^{19}F NMR (471 MHz, DMSO-d_6) of **4**.

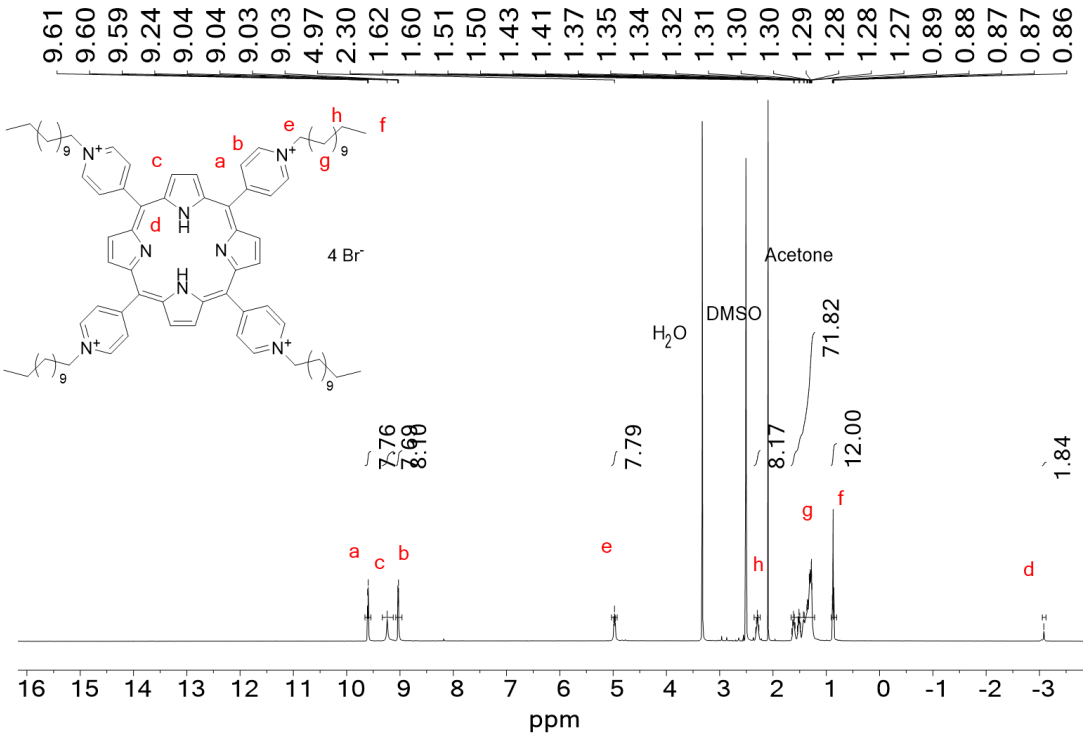

Figure S14. ^{1}H NMR (500 MHz, DMSO-*d*$_6$) of **5**.

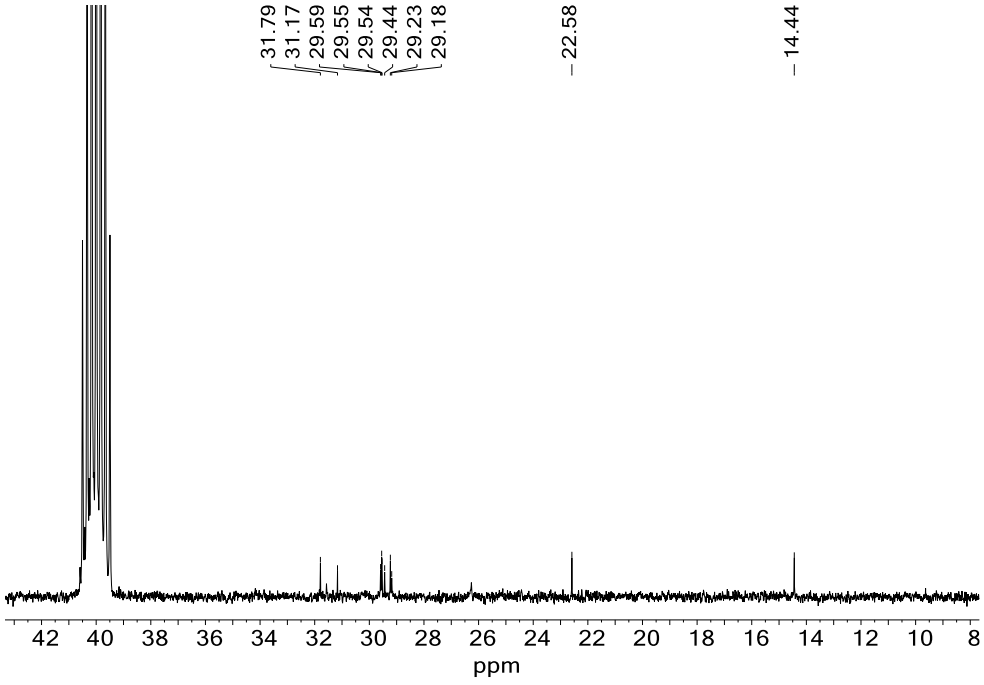

Figure S15. ^{13}C NMR (126 MHz, DMSO-*d*$_6$) of **5.**

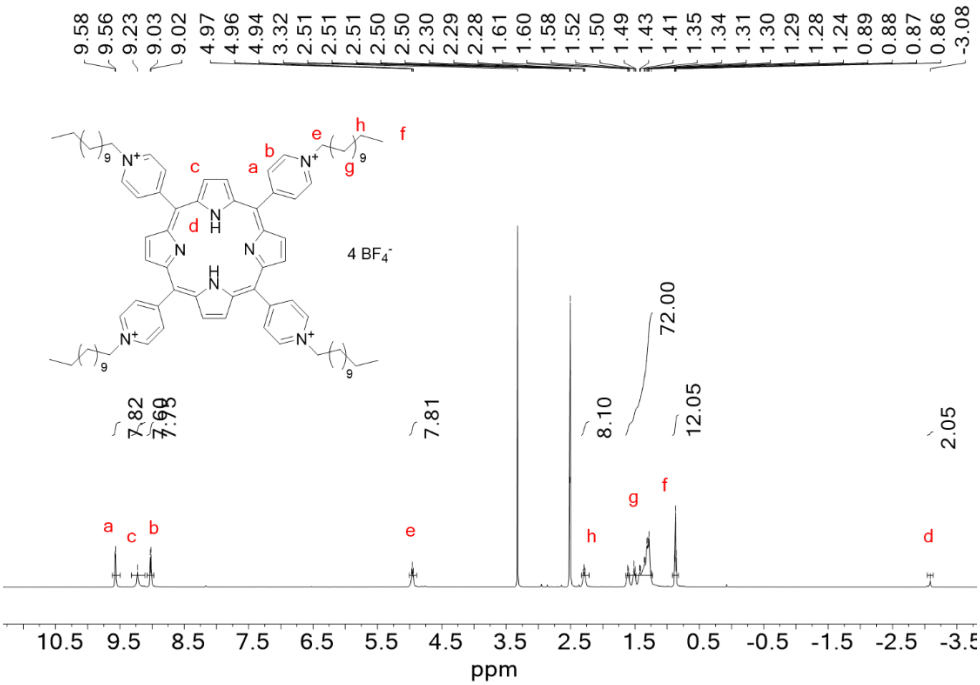

Figure S16. ^{1}H NMR (500 MHz, DMSO-d_6) of **6**.

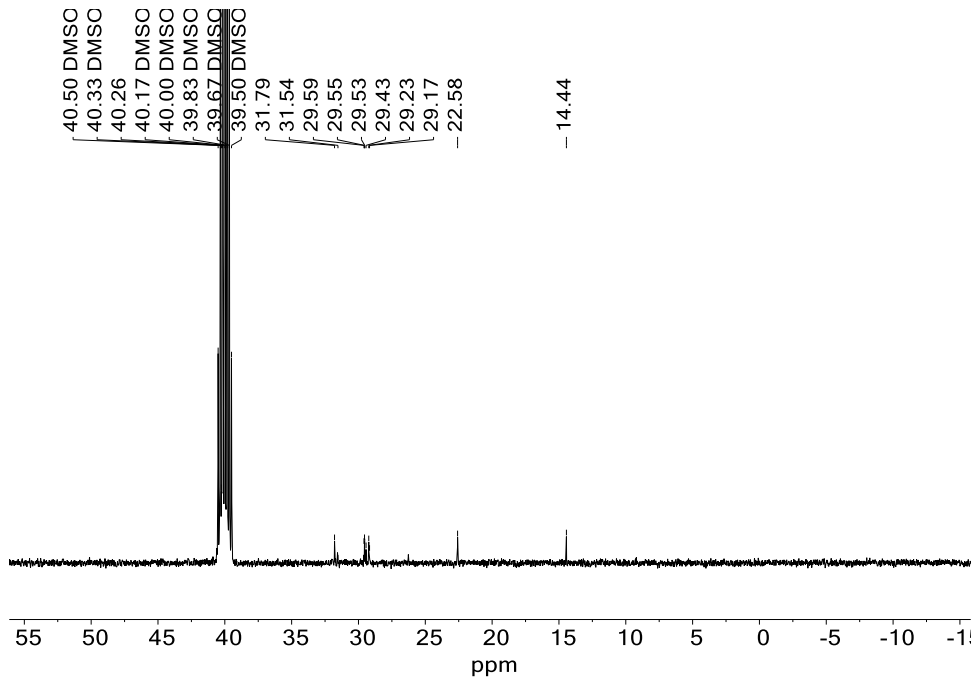

Figure S17. ^{13}C NMR (126 MHz, DMSO-d_6) of **6.**

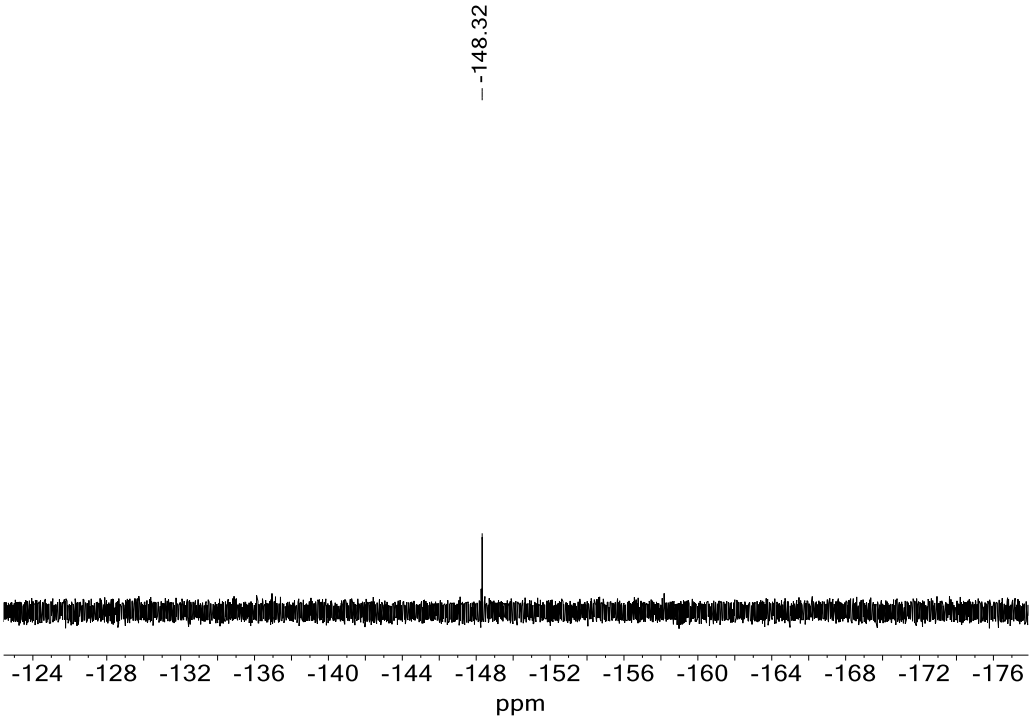

Figure S18. ^{19}F NMR (471 MHz, DMSO-d_6) of **6**.

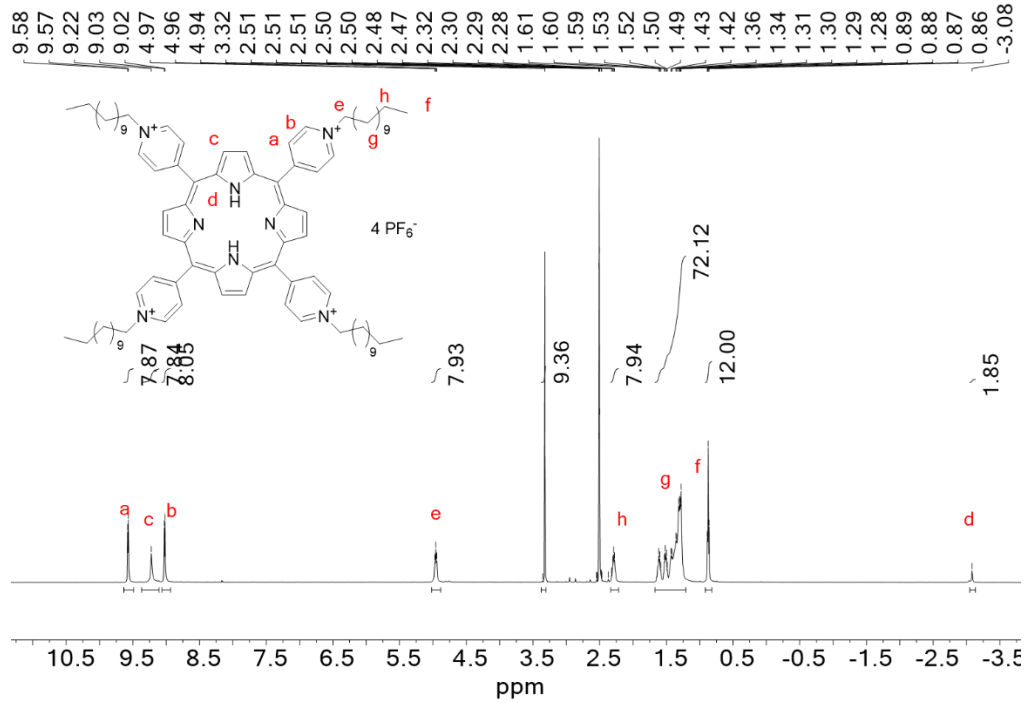

Figure S19. ^{1}H NMR (500 MHz, DMSO-d_6) of **7**.

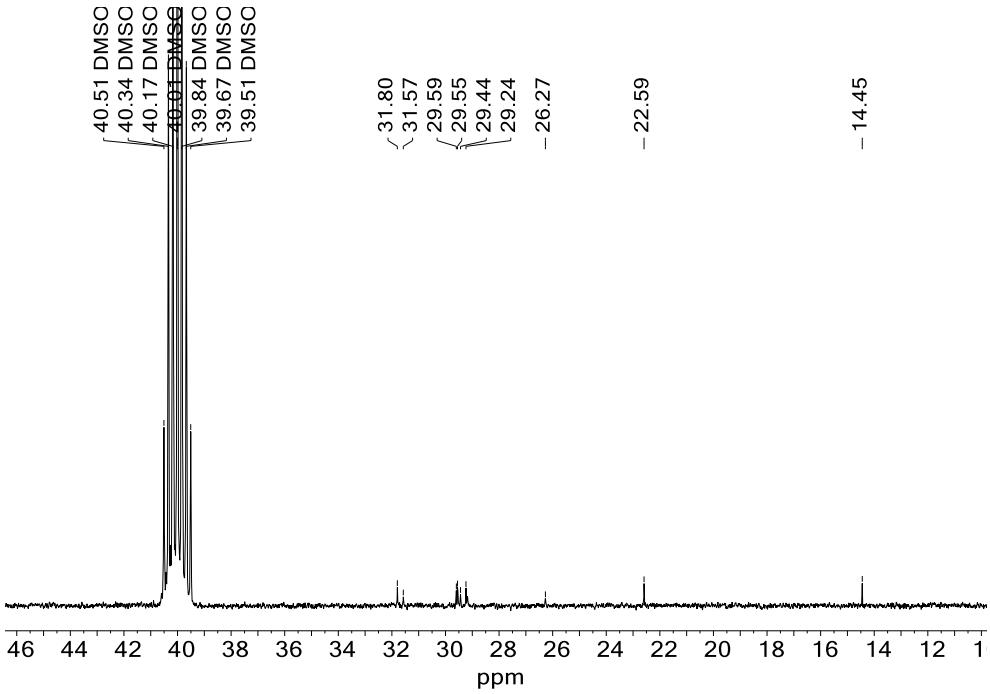

Figure S20. ^{13}C NMR (126 MHz, DMSO-d_6) of **7.**

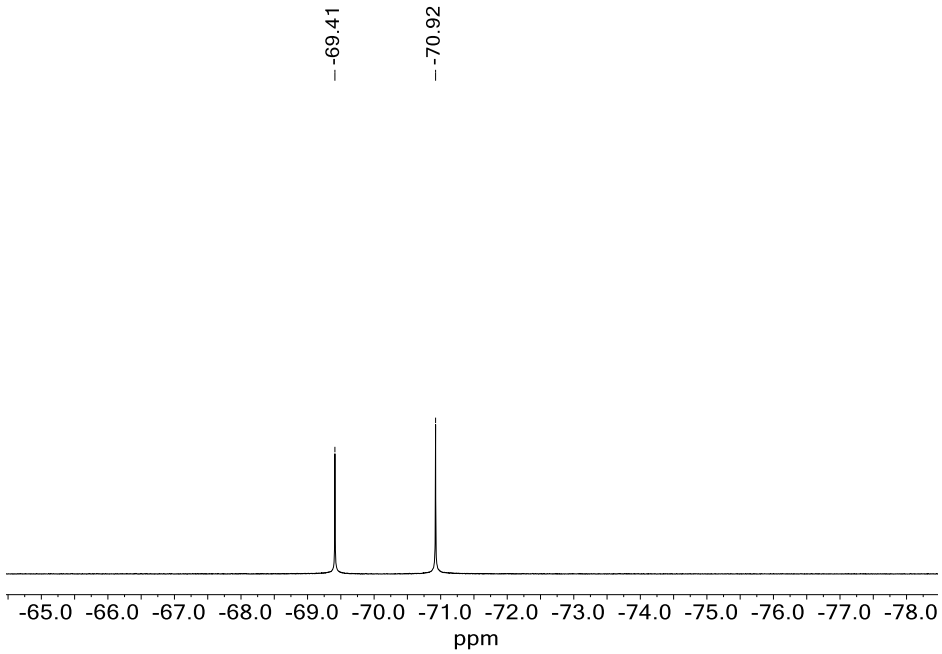

Figure S21. ^{19}F NMR (471 MHz, DMSO-d_6) of **7**.

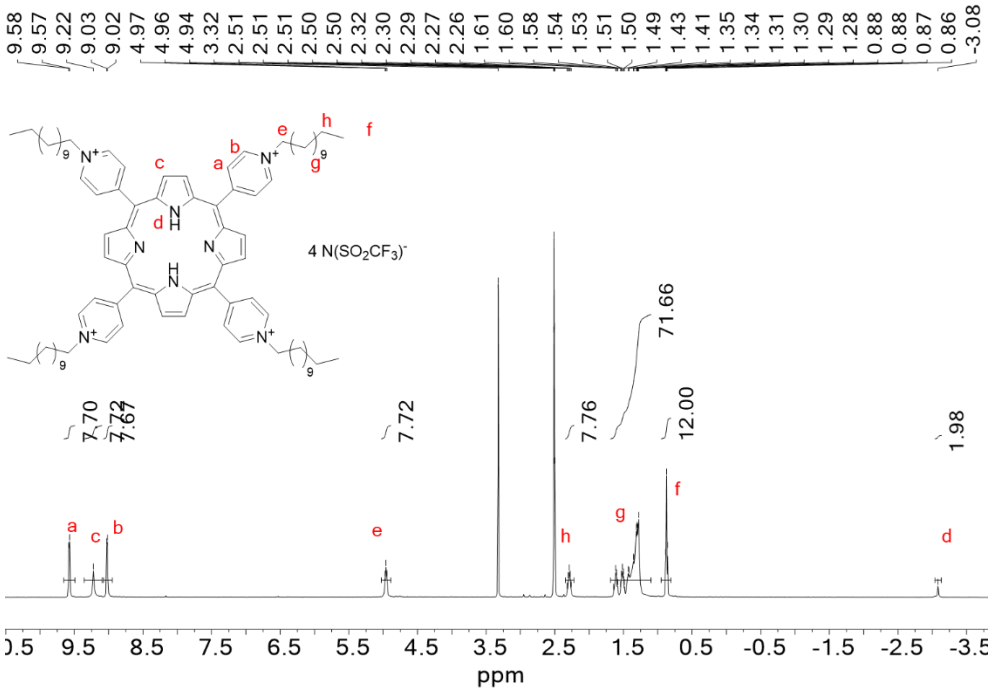

Figure S22. ^{1}H NMR (500 MHz, DMSO-d_6) of **8**.

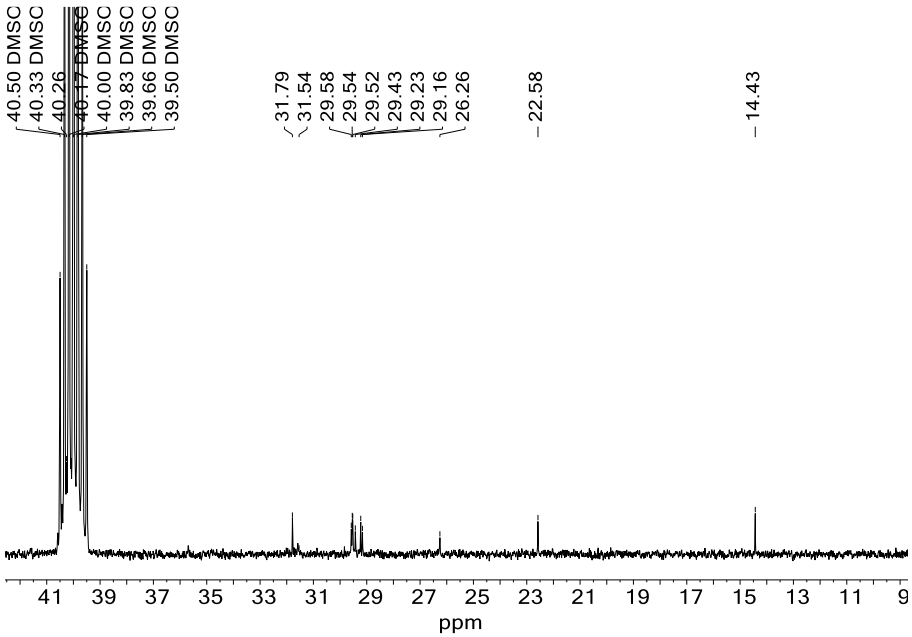

Figure S23. ^{13}C NMR (126 MHz, DMSO-d_6) of **8.**

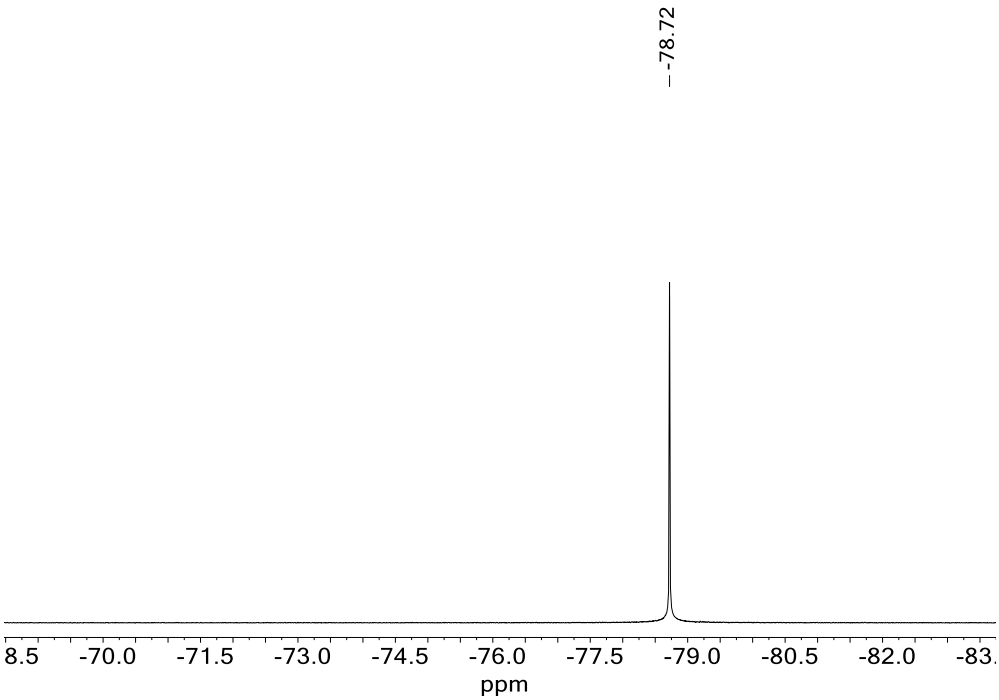

Figure S24. ^{19}F NMR (471 MHz, DMSO-d_6) of **8**.

Fourier Transform Infrared Spectroscopy **(FT-IR)**. FT-IR spectra were recorded using a Bruker Alpha FT-IR instrument, Bruker Optics Inc. (Billerica, MA) with an attenuated total reflection (ATR) sampler equipped with a diamond crystal. Spectra were obtained in the range of 4000-400 cm^{-1} with 4 cm^{-1} resolution.

Characteristic P-F stretching and bending signals at 830 and 553 cm^{-1} of the compounds containing $[PF_6]^-$ (**3** and **7**) were detected.[2] Similarly, the characteristic bands of $[BF_4]^-$ (B-F, 1052 cm^{-1})[2] and $[NTf_2]^-$ (S=O stretching at 1350, 1330, and 1052 cm^{-1}, C-F stretching at 1175 and 1135 cm^{-1}, and S-N-S stretching at 610, 570, and 510 cm^{-1})[3] were detected after anion exchange, suggesting the anion exchange was successful.

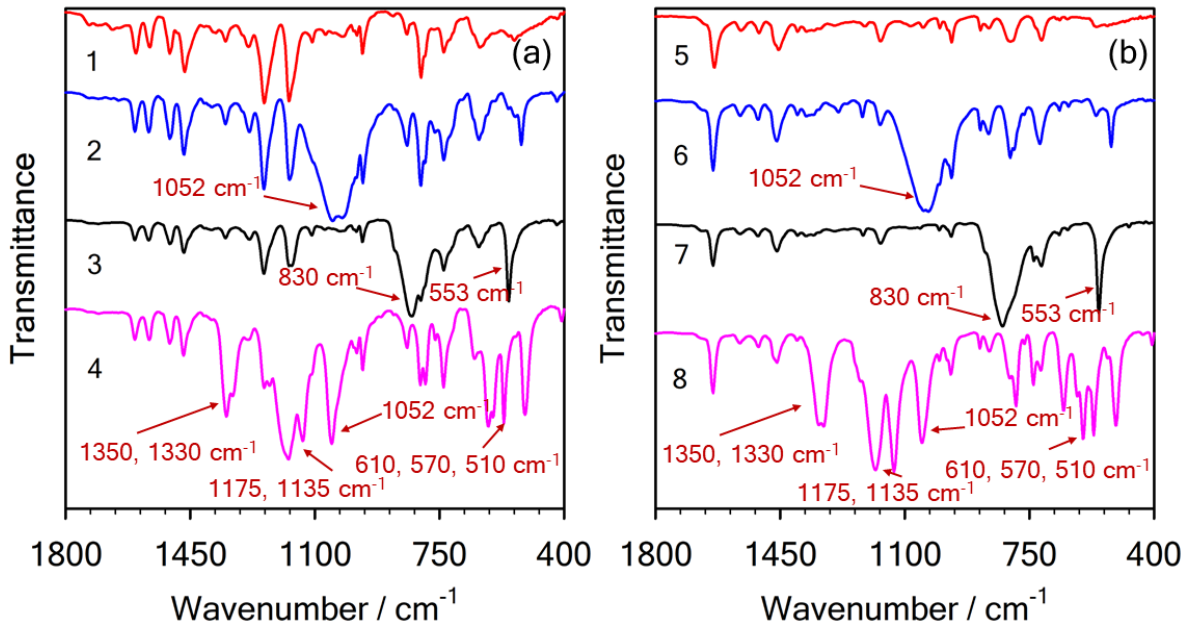

Figure S25. FT-IR results of porphyrin salts.

High Resolution Mass Spectroscopy (HRMS)*:* HRMS was run on an Exactive Plus Orbitrap mass spectrometer (Thermo Scientific, Waltham, MA) with an electrospray ion source (electrospray ionization) using loop injection with 5µL methanol solution.

Thermogravimetric Analysis (TGA)*:* Thermogravimetric analyses (TGA) were conducted with a TGA 5500 (TA Instruments Ltd., New Castle, DE). The instrument's internal temperature was calibrated by observing the melting points of Au, Zn, and In. Samples of 2-10 mg were analyzed in 100 µL platinum pans under N_2 atmosphere. All samples were heated from room temperature to 75 °C with a 30 min isotherm at 75 °C in order to remove excess volatiles or residual solvents. After the isotherm, samples were heated to 700 °C at a heating rate of 5 °C min^{-1}, then held at 700 °C for 30 min. Decompositions temperatures were recorded as the onset to 5% mass loss ($T_{5\%dec}$).

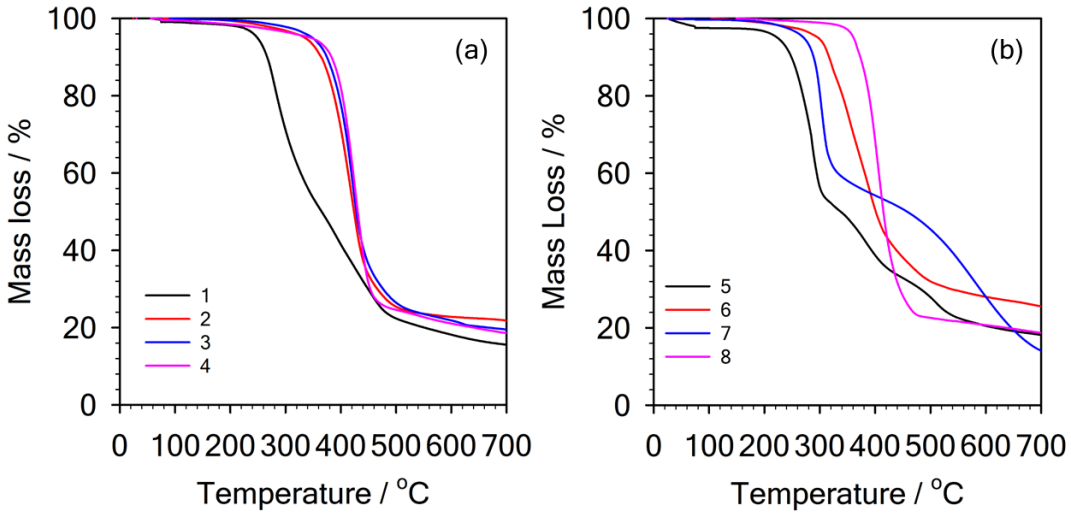

Figure S26. TGA of porphyrin salts.

Differential Scanning Calorimetry (DSC): DSC studies were conducted with a DSC 2500 (TA Instruments Ltd., New Castle, DE). Samples of 2-10 mg were analyzed in 100 µL Aluminum Tzero pans under nitrogen atmosphere. All samples were heated from -90 °C to 50 °C below their decomposition temperature ($T_{5\%dec}$ from TGA) at 10 °C min^{-1}, then cooled down to -90 °C and marked as one cycle. Three cycles were done for each sample.

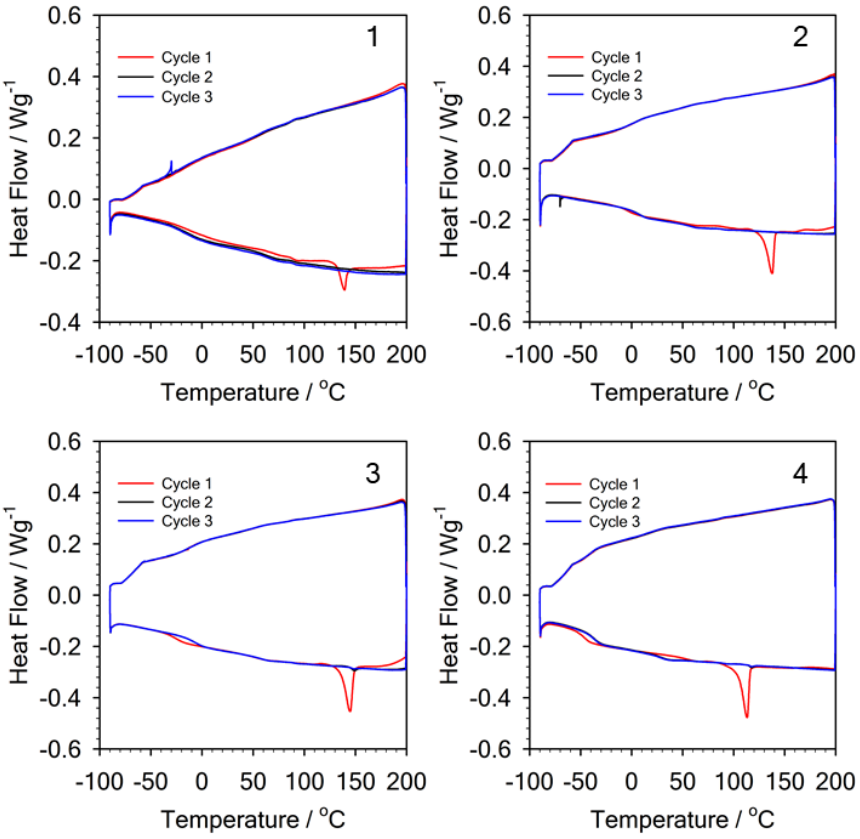

Figure S27. DSC of TOHPP-based porphyrin salts.

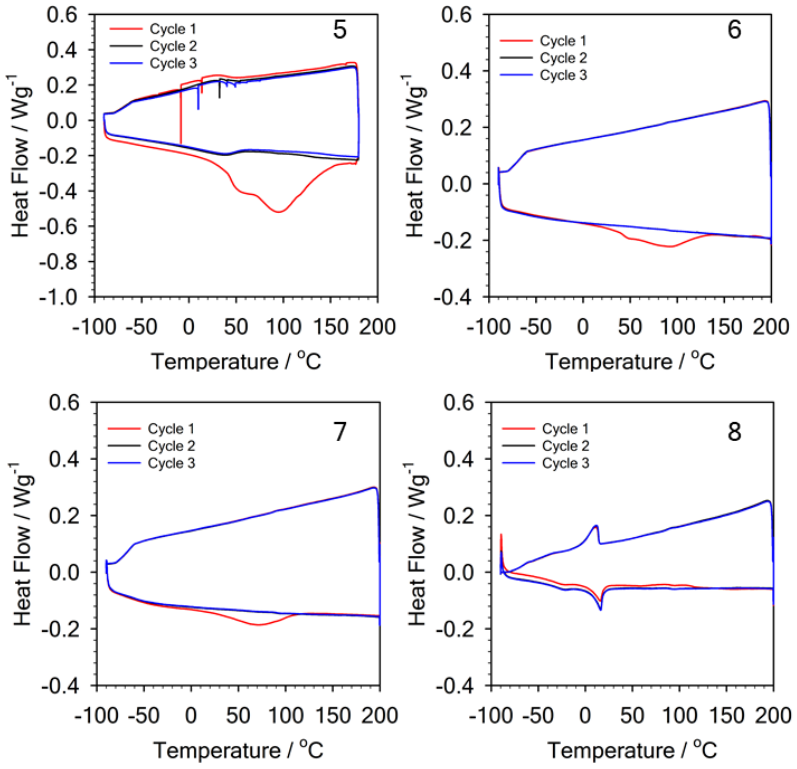

Figure S28. DSC of T4PyP-based porphyrin salts.

Single Crystal X-ray Diffraction (SCXRD): SCXRD data for **a** and **8**·4$C_6H_5NO_2$ were collected on a Bruker D8 Advance diffractometer with a Photon 100 CMOS area detector and an IμS microfocus X-ray source (Madison, WI) using Cu-*K*α radiation. Crystals were coated with Paraffin oil and cooled to 100 K under a cold stream of nitrogen using an Oxford cryostat (Oxford Cryosystems, Oxford, UK). The Apex3 software suite (Madison, WI), was used for data collection, reduction, and unit cell assignment. The crystals were solved using an iterative dual space approach as implemented in SHELXT.[4] Non-hydrogen atoms were located from the difference map and refined anisotropically. Hydrogen atoms bonded to their carrier atom were placed in calculated positions. All hydrogen atom coordinates and thermal parameters were constrained to ride on the carrier atoms.

The porphyrin structure **8**·4$C_6H_5NO_2$ **(Figure S29)** has a large amount of disorder in the structure, for example, one of the side-chains of the porphyrin molecule is disordered in which it was not successfully modeled. Other major disorder was observed for one of the $[NTf_2]^-$ anions, which was modeled and refined isotropically, to form two *cis* conformers and one *trans*

conformations. The *cis*:*cis*:*trans* conformer occupancies were found to be approximately 45:35:20, respectively.

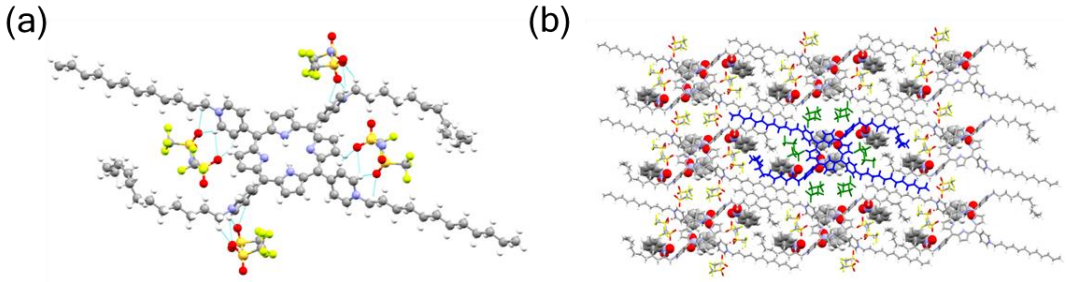

Figure S29. (a) Location of the anions around the porphyrin cation forming C-H···O interactions depicted in blue dashed lines. (b) Crystal packing of **8**·4$C_6H_5NO_2$ along the a-axis; the nitrobenzene is depicted in spacefill, while one of the porphyrin cations is highlighted in blue and the anions surrounding it in green.

The crystal structure of 1-(12-bromododecyl)-3-ethylimidazolium bromide (**a**) crystallizes in the monoclinic space group $P2_1$ (**Fig. S30a**). The unit cell consists of two different imidazolium cations and two bromide anions. Each bromide anion is surrounded by three imidazolium cations through weak C-H···Br contacts, with shortest narrows of 2.608(1) and 2.648(1) Å, formed between the imidazolium C2 acidic hydrogen and Br-anion.

On the other hand, the imidazolium cations in **a** are surrounded by four bromide anions. Yet, the two cations differ from each other through the torsion angles calculated as C2-N-C_{chain}-C_{chain} of 94.56 and -129.63°.The overlay of the two imidazolium cations are showing in **Fig. S30b**, which exhibit the different orientations of the alkyl-chains.

Interestingly, the packing in **a** shows that the covalent bonded Br-atoms at the terminal position of the alkyl chain are forming very weak C-H···Br, holding two near cations in head-to-tail fashion along the crystal lattice. The alkyl chains are forming apolar domain (**Fig. S30c**), while the imidazole rings and the anions are forming the polar domains. The imidazolium cations in **a** are oriented in zigzag fashion, in contrast to the crystal structure of 1-hexadecyl-3-methyl-imidazolium bromide monohydrate reported by Zhang and co-workers,[5] in which the imidazolium cations are organized in parallel blocks along the lattice.

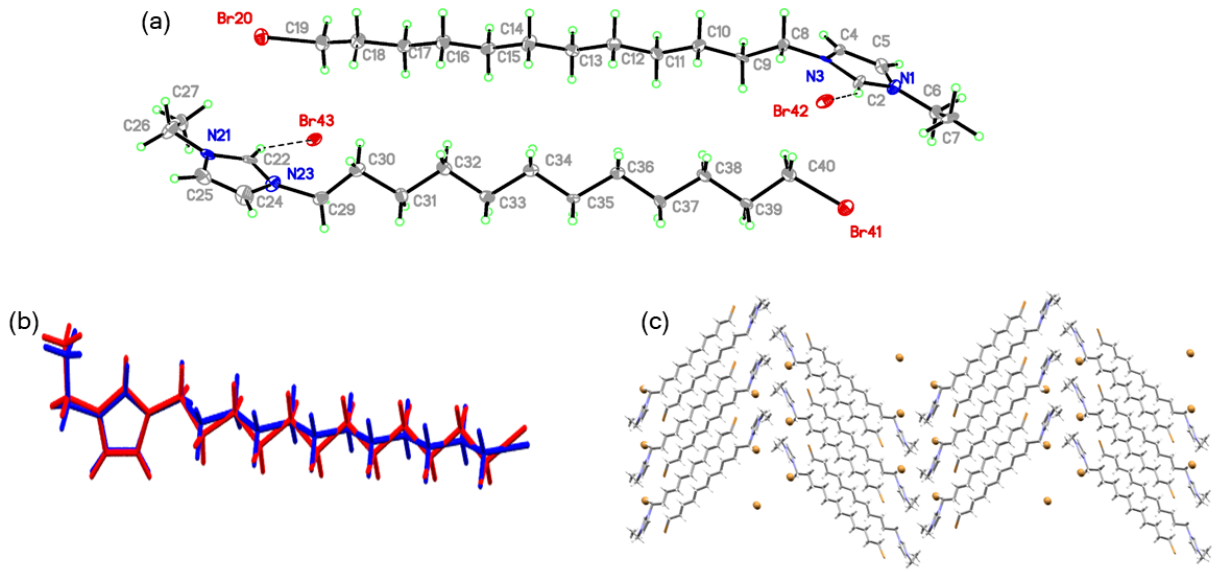

Figure S30. (a) crystal structure of a, (b) Cation overlay in a exhibits clear differences in the orientations of the alkyl groups, (c) Crystal packing of a along the crystallographic c-axis.

Solubility Test: Saturated solutions were prepared by dissolving a certain amount of sample (ca. 4 mg) in 400 µL solvent and shaking for 1 h at room temperature. Then, the solution was centrifuged (Thermo Scientific Sorvall Legend XF, Waltham, MA) at 3500 rpm for 10 min. If fully dissolved, more sample was added until it became saturated. The supernatant was diluted 10-1000 times with the same solvent depend on the concentration and analyzed by UV-Vis spectrometer. The solubilities were determined by UV-Vis using calibration curves.

Ultraviolet–visible (UV-Vis) spectra: UV-Vis spectra of the solutions were recorded in the range of 350-650 nm using a UV/Vis Spectrophotometer (Thermo Scientific, Evolution 260 Bio, Waltham, MA) with 1 cm path length quartz cuvette.

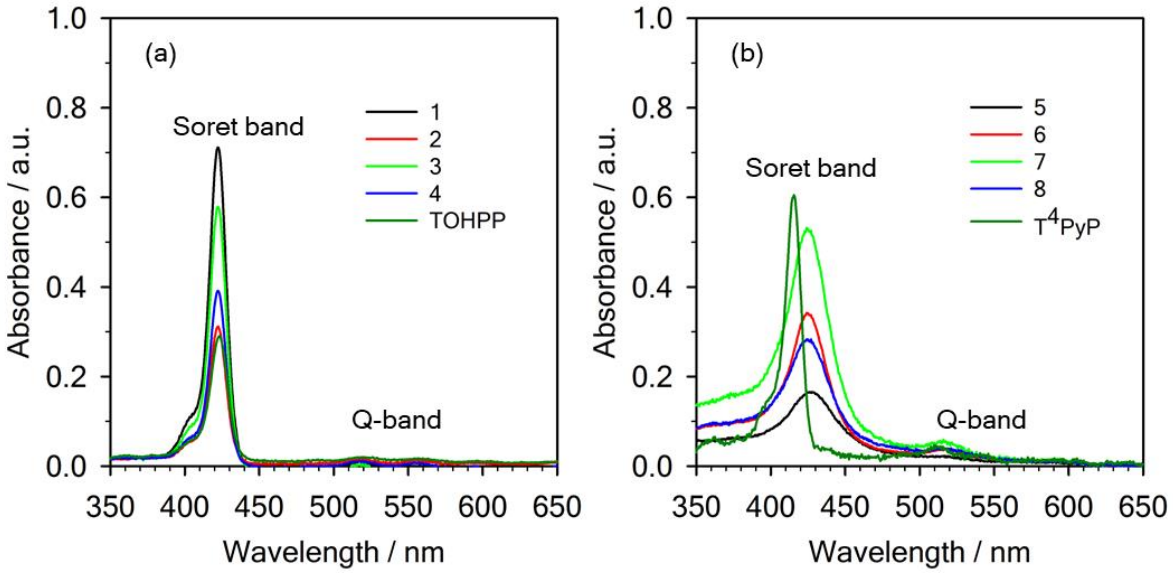

Figure S31. UV-Vis spectra of porphyrin-based compounds in DMF. (a) TOHPP-based compounds, (b) T^4PyP-based compounds.

Table S1. Soret band and Q band of porphyrins

Sample	Soret band (nm)	Q band (nm)
TOHPP		
1		
2	423	518, 556, 594, 548
3		
4		
T^4PyP	415	512, 544, 575, 607
5		
6	424	517, 550, 588, 617
7		
8		

Singlet Oxygen Quantum Yield (Φ_Δ): Singlet oxygen quantum yield was tested by photooxidation of 9,10-dimethylanthracene (DMA) in DMF with *meso*-tetraphenylporphyrin (TPP) as a standard (Φ_Δ = 0.62).[6] 3 mL of DMA solution (0.9×10^{-4} M) was mixed with 0.2 mL porphyrin solution (1.2×10^{-5} M) or TPP (1.2×10^{-5} M) in a 1-cm quartz cuvette and the cuvette was irradiated with an illuminator (Cole Parmer Industries Inc., USA) equipped with a 150 W halogen lamp. After irradiation for different times (up to 10 min), UV-Vis spectra were recorded and the kinetics of DMA photooxidation was calculated using the absorbance at 379 nm. The observed rate constants (k) were calculated by a linear least-squares fit of the semilogarithmic plot of ln A_0/A versus time.

The singlet oxygen quantum yield (Φ_{Δ}) values were obtained by comparing the slope of the sample and reference. DMA solution (0.9×10^{-4} M) without photosensitizer was also studied by mixing with 0.2 mL DMF as a blank control experiment. All the tests were performed three times.

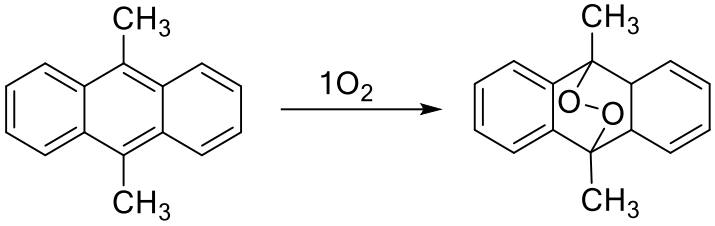

Scheme S1. Photooxidation of DMA by singlet oxygen ($^1O_2$).

References

[1] B. S. Lee, Y. S. Chi, J. K. Lee, I. S. Choi, C. E. Song, S. K. Namgoong, S.-g. Lee, *J. Am. Chem. Soc.* **2004**, *126*, 480-481.

[2] P. A. Z. Suarez, J. E. L. Dullius, S. Einloft, R. F. De Souza, J. Dupont, *Polyhedron* **1996**, *15*, 1217-1219.

[3] M. Herstedt, M. Smirnov, P. Johansson, M. Chami, J. Grondin, L. Servant, J. C. Lassègues, *J. Raman Spectrosc.* **2005**, *36*, 762-770.

[4] G. Sheldrick, *Acta Crystallographica Section C* **2015**, *71*, 3-8.

[5] Z. Wei, X. Wei, S. Fu, J. Liu and D. Zhang, *Acta Cryst. E* 2009, **65**, o1159.

[6] I. Scalise, E. N. Durantini, *J. Photochem. Photobiol. A: Chem.* **2004**, *162*, 105-113.